Giant Sensitivity of Optical Fiber Sensors by means of Lossy Mode Resonance

Authors: Francisco J. Arregui[1], Ignacio Del Villar[2,*], Carlos R. Zamarreño[1], Pablo Zubiate[1], Ignacio R. Matias[2]

Affiliations:

[1] Sensors Research Laboratory, Public University of Navarra, 31006 Pamplona, Spain

[2] Institute of Smart Cities, Jeronimo de Ayanz Center, Campus Arrosadia, 31006 Pamplona, Spain

*Corresponding author: ignacio.delvillar@unavarra.es

Telephone: +34948169256

Fax: +34948169720

Email addresses of rest of authors:

Francisco J. Arregui: parregui@unavarra.es

Carlos R. Zamarreño: carlos.ruiz@unavarra.es

Pablo Zubiate: pablo.zubiate@unavarra.es

Ignacio R. Matias: natxo@unavarra.es

Abstract: Here we show an optical refractometer with a giant sensitivity of 304,360 nm per refractive index unit (nm/RIU). This sensitivity corresponds to a resolution of 3.28 x 10^{-9} RIU if a standard optical spectrum analyzer with a resolution of 1 pm is used. This record sensitivity is obtained by means of a Lossy Mode Resonance (LMR) optical fiber sensor in a surrounding media with refractive index around 1.45. This achievement implies that the utilization of the LMR phenomenon opens the door to devices and systems that can beat, in terms of sensitivity, those used currently in real-time biomolecular analysis such as Surface Plasmon Resonance (SPR) devices.

Keywords: D-shaped fiber, lossy mode resonance, optical fiber sensor, refractometer

1. INTRODUCTION

In the literature, little attention has been paid to waveguides deposited with nanocoatings of moderate optical absorbance (lossy materials), and metal-clads [1-3]. This is easy to understand because, in order to achieve long distance communications, an optical medium with negligible absorbance is pursued [4]. Just the opposite is intended in Surface Plasmon Resonance (SPR) devices where metallic thin films coat the optical waveguide [5]. Lossy Mode Resonances (LMRs) just stand in the middle of these two extreme situations [6]. The basis of this resonance is that a particular mode guided in the waveguide (e.g. an optical fiber) experiences a transition to guidance in the moderate absorbing submicron or nanometric scale coating at a certain wavelength. Due to the complex refractive index of the coating, the effective index of the mode is also complex (it presents a not negligible imaginary part). Consequently, it can be considered as a lossy guided mode or, in a more simple way, a lossy mode [4-6]. There are some authors that have used the generic term “guided mode” resonance for this phenomenon [7], but a lossy mode is a specific type of guided mode and, due to this, the term Lossy Mode Resonance has been adopted in the last six years since the first proposal of LMR based devices for sensing [6,8-10]. LMRs have been often confused with surface plasmon resonances (SPRs) in the past by many groups, including ourselves, because both phenomena present a similar shape in the

optical spectrum [11-13]. This controversy has been recently solved thanks to one work that permits to observe an SPR and an LMR separately with the same experimental setup [14]. Later on, it has been possible to analyze the sensitivity of both SPR and LMR resonances in the same spectrum [15]. The material used for the thin-film was Indium Tin Oxide (ITO), which at shorter wavelengths satisfies the conditions for generation of LMRs (i.e. the real part of the thin-film permittivity is negative and higher in magnitude than both its own imaginary part and the permittivity of the material surrounding the thin-film), and at longer wavelengths the conditions for generation of SPRs (i.e. the real part of the thin-film permittivity is positive and higher in magnitude than both its own imaginary part and the material surrounding the thin-film) [7]. That is why the indication in some works that ITO can be used for generation of SPRs [16,17], is not in contradiction with the ability of the same material to be used for generation of LMRs.

In fact, LMRs show some clear differences with respect to SPR: the central wavelength of the optical resonance and the sensitivity can be easily adjusted as a function of the thickness and refractive index of the lossy thin film [6,18]. Moreover, there is a remarkable peculiarity with respect to SPR: the optical resonance in LMRs can be observed for both TM and TE polarizations [19].

In this work, we prove that the combination of a D-shaped optical fiber coated with a nanometric scale metal oxide permits indeed high sensitivities both for refractive indices approaching the refractive index of fused silica, and for the water refractive index region. The phenomenon has been studied numerically and demonstrated experimentally as well.

2. MATERIALS AND METHODS

The experimental setup is depicted in Fig. 1. Light from a broadband multi-LED light source HP 83437A is transmitted through a thin-film coated D-shaped fiber. The output of the fiber is connected to an optical spectrum analyzer (OSA) HP 86142A that permits to monitor a wavelength range from 1150 to 1680 nm. In order to control the polarization of light, a

depolarizer from Phoenix Photonics and a polarization controller (Agilent 9169A) are included between the broadband source and the fiber.

The D-shaped optical fiber (from Phoenix Photonics LTD) consists of a standard single mode fiber Corning® SMF-28 with a side-polished length of 1.7 cm (see detail in Fig. 1).

The optical fiber polished length, henceforward called sensitive region, is coated with a thin film by means of a DC sputter machine (ND-SCS200 from Nadetech S.L.). Two different materials for the target were used: ITO and SnO_2. Both of them present a 99.99% of purity and were purchased from ZhongNuo Advanced Material Technology Co. The parameters used in the experiment were: partial pressure of argon of 9×10^{-2} mbar and intensity 150 mA.

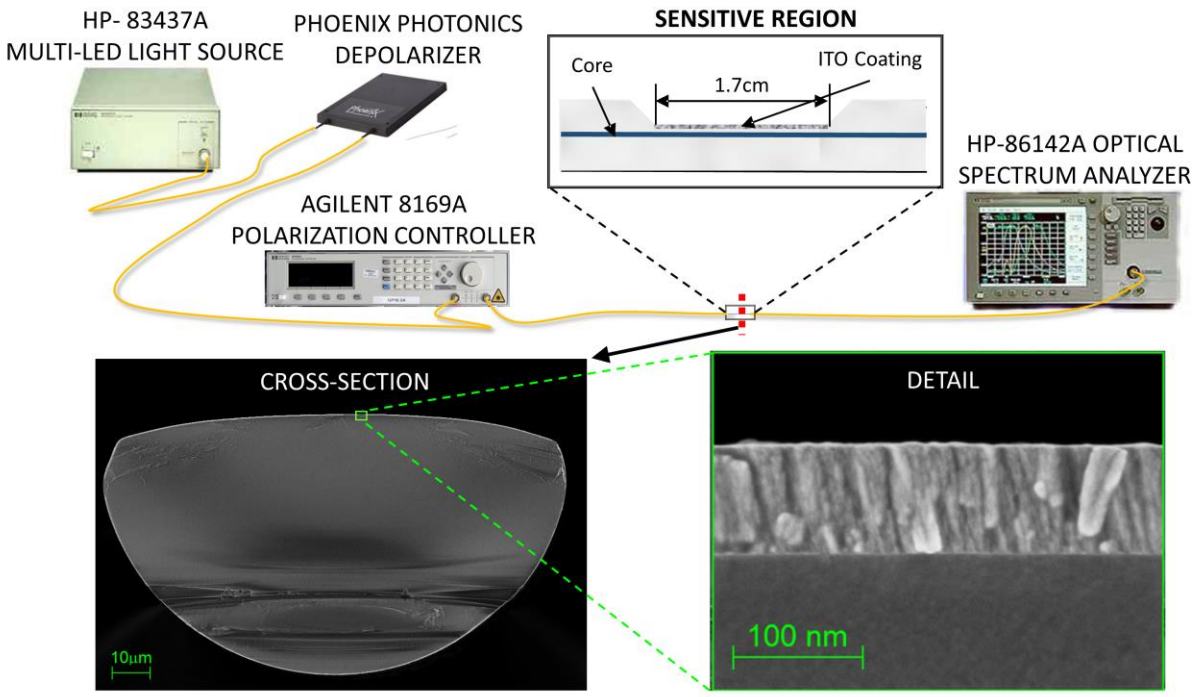

Fig. 1. Experimental setup. The system is composed of a multi-LED source, a depolarizer, and polarization controller, which permits to excite the D-shaped fiber with a TE or a TM polarized signal, and an optical spectrum analyzer that monitors the optical spectra. The D-shaped fiber is side polished in a region of 1.7 cm, where a thin-film of ITO or SnO_2 is deposited.

For the characterization of the ITO thin-film an ellipsometer UVISEL, with spectral range 0.6-6.5 eV (190 – 2100 nm), an angle of incidence 70°, an spot size 1 mm and Software DeltaPsi2TM (from Horiba Scientific Thin Film Division) was used. The wavelength dependence of ITO thin-film refractive index and extinction coefficient can be seen in Fig. 2.

The optical fiber cladding, made of fused silica, has been estimated with the Sellmeier equation:

$$n^2(\omega) = 1 + \sum_{j=1}^{m} \frac{B_j \omega_j^2}{\omega_j^2 - \omega^2} \qquad (1)$$

with parameters: B_1=0.691663, B_2=0.4079426, B_3=0.8974794, λ_1=0.0684043 µm, λ_2= 0.1162414, and λ_3= 9.896161, where $\lambda_j = 2\pi c/\omega_j$ and c is the speed of light in vacuum [20]. The optical fiber core refractive index for the simulations has been obtained, according to the specifications from Fibercore Inc for SMF28, by increasing the refractive index of the cladding 0.36%.

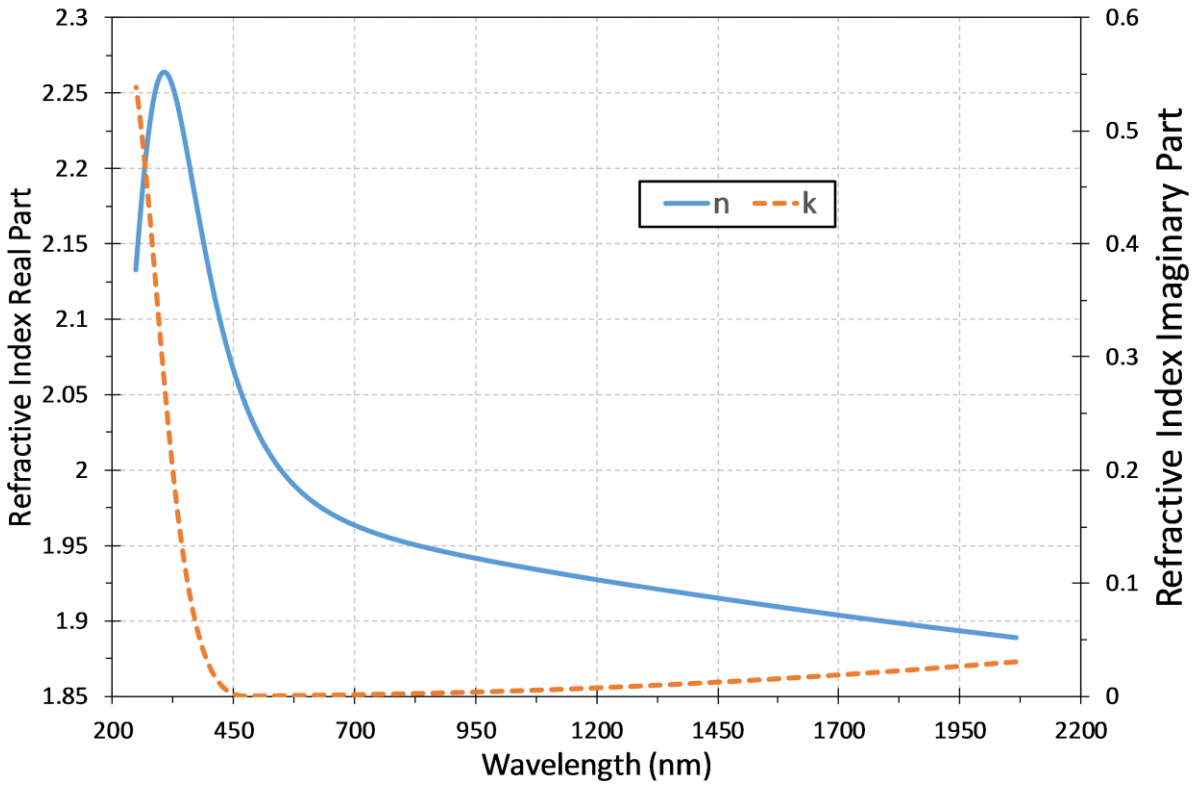

Fig. 2. Index of refraction and extinction coefficient (n,k) of ITO deposited layer.

Refractive index measurements from glycerol solutions were taken with a refractometer 30GS from Mettler Toledo Inc. This device obtains the refractive index for a wavelength of 589.3 nm. The refractive index of water at this wavelength is 1.333. However, according to [21], the refractive index of water is 1.321 at 1400 nm, the central wavelength of the range explored in our experiments. The same offset observed for water is obtained for glycerol if the values obtained at 589.3 nm are compared to those obtained at 1293 nm [22]. Consequently, this offset will be applied to all measurements taken by the refractometer for the glycerol solutions studied henceforward. Due to the high resolution of the D-shaped fiber based sensor, its value is limited to the resolution of the Mettler Toledo Refractometer that we use for calibration, which is a fourth decimal in refractive index. Regarding measurement errors, they are negligible due to the parabolic approximation used to obtain the central wavelength of the LMR.

FIMMWAVE® is used for analyzing the transmission through the ITO nanocoated D-shaped fiber. The propagation is obtained with FIMMPROP, a module integrated with FIMMWAVE. Three sections are defined: an SMF segment, a side polished SMF segment and another SMF segment. For the SMF segment the finite difference method FDM is used because it is the most accurate method available for a cylindrical waveguide, whereas for the side polished SMF segment, with a more complex profile, the FEM Solver, based on the finite-element method, is used. This solver can put mesh points on the material boundaries, whereas the FDM Solver has a rigid mesh that in general does not coincide with the material boundaries. The number of modes analyzed in the SMF section is 1 because light in guided through the core, whereas in the side polished SMF 20 modes are analyzed.

3. RESULTS AND DISCUSSION

As it was indicated previously, LMRs can be obtained for both TE and TM polarization. For the sake of simplicity and in order to underline that it is not an SPR, the TE polarization case will be analyzed henceforward. The sensitive region of the LMR device is immersed in deionized ultrapure water (RI=1.321) and the experimental spectrum is also plotted in Fig. 3a. Both numerical and experimental curves agree.

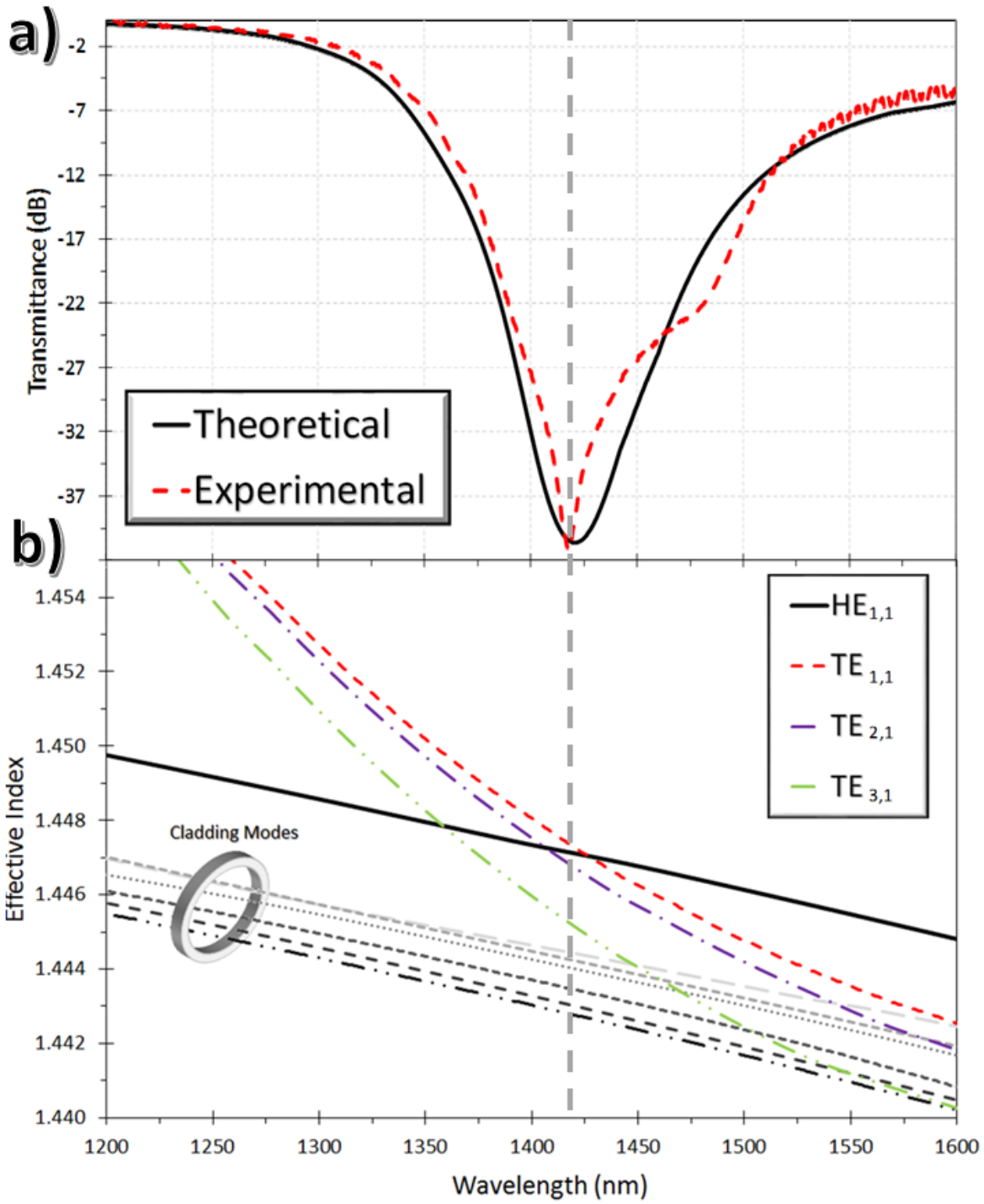

Fig. 3. (A) Numerical and experimental optical spectrum obtained with a D-shaped fiber coated with a 92 nm ITO layer. **(B)** Effective index of modes: the LMR is centered at 1420 nm and the effective index real part of modes $TE_{1,1}$, $TE_{2,1}$ and $TE_{3,1}$ experience a transition to guidance in the ITO layer in the LMR wavelength range.

The generation of this resonance can be explained by analyzing the mode effective index as a function of wavelength in Fig. 3b. $HE_{1,1}$ is the fundamental mode (the mode guided in the core), and $TE_{1,1}$, $TE_{2,1}$ and $TE_{3,1}$ are the modes guided in the ITO coating, following the notation used for rectangular waveguides (if the polarization was TM, then $TM_{1,1}$, $TM_{2,1}$ and $TM_{3,1}$, modes would be guided in the thin-film). Approximately at 1400 nm, $TE_{1,1}$, $TE_{2,1}$ and $TE_{3,1}$, experience a transition to guidance in the thin-film, which coincides with the position of the resonance and agrees with other works indicating that LMR occurs at near cutoff condition [2,6].

The imaginary part of the effective index of $HE_{1,1}$, $TE_{1,1}$, $TE_{2,1}$ and $TE_{3,1}$ can be observed in Fig. 4. According to the real part of the effective index, the imaginary part of the effective index of $TE_{1,1}$, $TE_{2,1}$ and $TE_{3,1}$ increases constantly as it is progressively guided from longer to shorter wavelengths. Consequently, the imaginary part of their effective index increases constantly. However, $HE_{1,1}$ is the core mode and is not guided in the thin-film. According to [23], during the transition to guidance of a mode to a thin-film, the rest of modes of the optical substrate experience a perturbation that affects the real and imaginary part of their effective index. That is why $HE_{1,1}$ increases its imaginary part during the transition of $TE_{1,1}$, $TE_{2,1}$ and $TE_{3,1}$, whereas $TE_{1,1}$, $TE_{2,1}$ and $TE_{3,1}$ just transit to a high imaginary refractive index. In view that the D-shaped region ends in a SMF region, light detected in the OSA corresponds with the core mode $HE_{1,1}$. Consequently, a lower optical transmission is obtained in the LMR spectral range.

In order to know the influence of the ITO coating thickness and length, and the influence of the thickness of the cladding region between the core and the ITO coating, some additional simulations have been performed. In Fig. 5, we use the same parameters as those used in Fig. 3 except for the cladding region. We compare three values: 5.2, 4.7 and 4.2 μm, and it can be observed that the resonance depth is increased as a function of a decreasing cladding region. In addition to this, several lengths have been studied for a cladding region of 5.2 μm: 2 mm, 6 mm, 12 mm and 17 mm. The variation of the length plays no role on the shape of the resonance. The resonance depth just increases as a function of the length. This indicates the LMR is not an interferometric phenomenon.

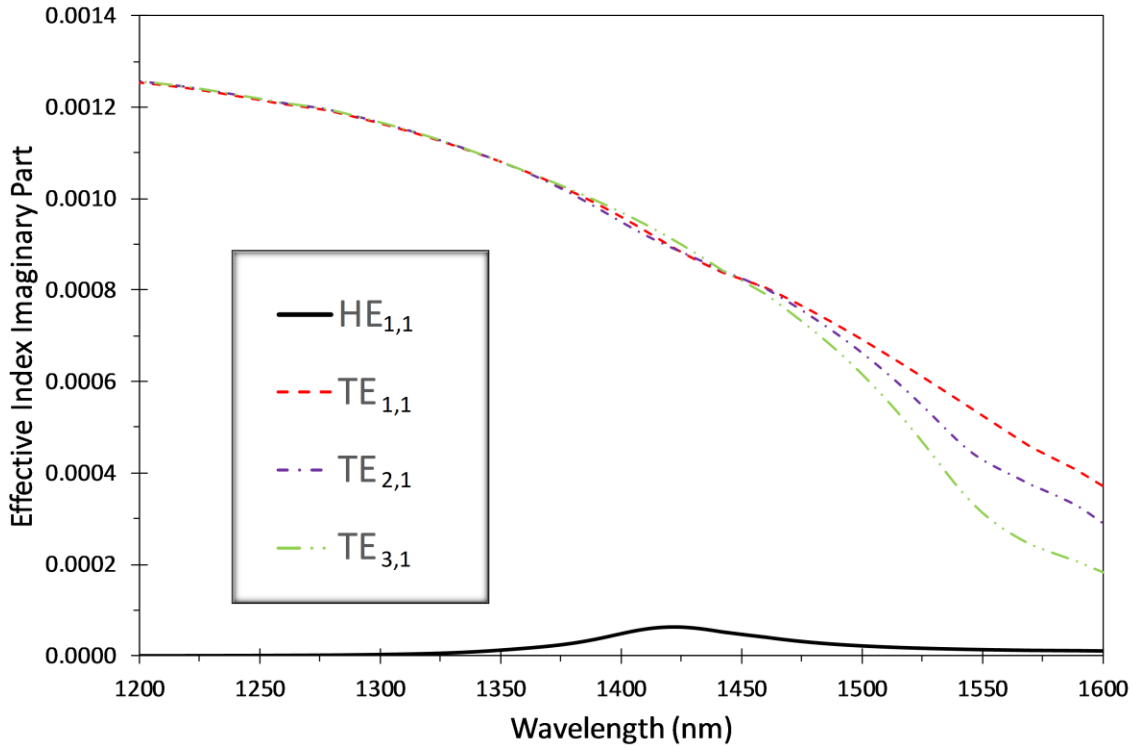

Fig. 4. Imaginary part of the effective index of the $HE_{1,1}$ (it shows a maximum a the central LMR wavelength: 1420 nm) and $TE_{1,1}$, $TE_{2,1}$, $TE_{3,1}$ (they experience a transition to guidance in the ITO layer in the LMR wavelength range).

The previous two variables permit to control the depth. However, the ITO coating thickness rules the spectral position of the resonance. In Fig. 6, several thickness values are explored: 80, 85, 90, 95, 100 and 250 nm. The last value has been selected to shift the resonance to wavelengths that cannot be tracked in the OSA. Thanks to this, we can see that the coating absorption is below 0.2 dB, negligible if compared with the LMR.

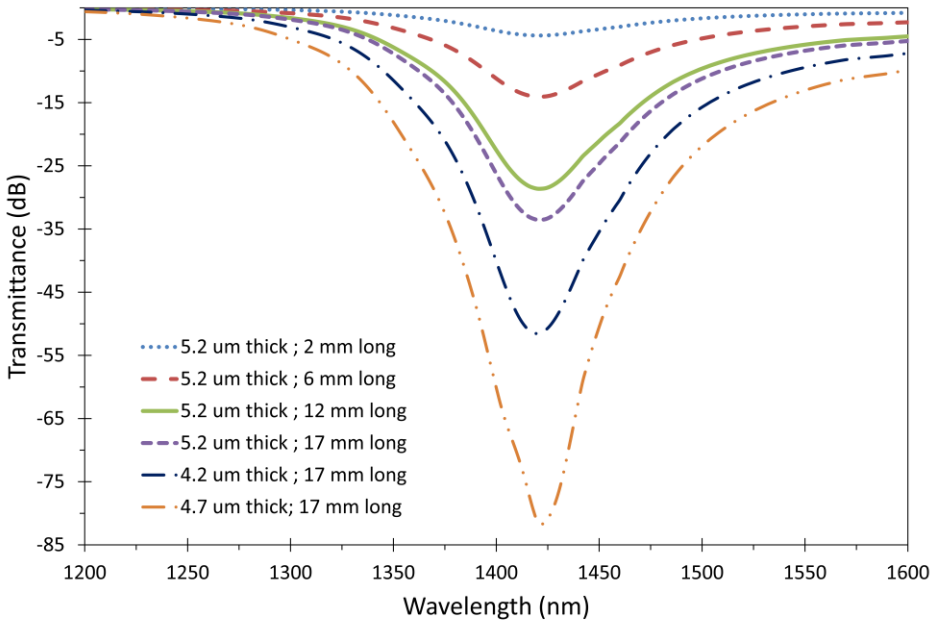

Fig. 5. Numerical spectra for different thickness values of the cladding region between the core and the ITO coating and for different ITO coating lengths. ITO thickness 92 nm and SRI= 1.321.

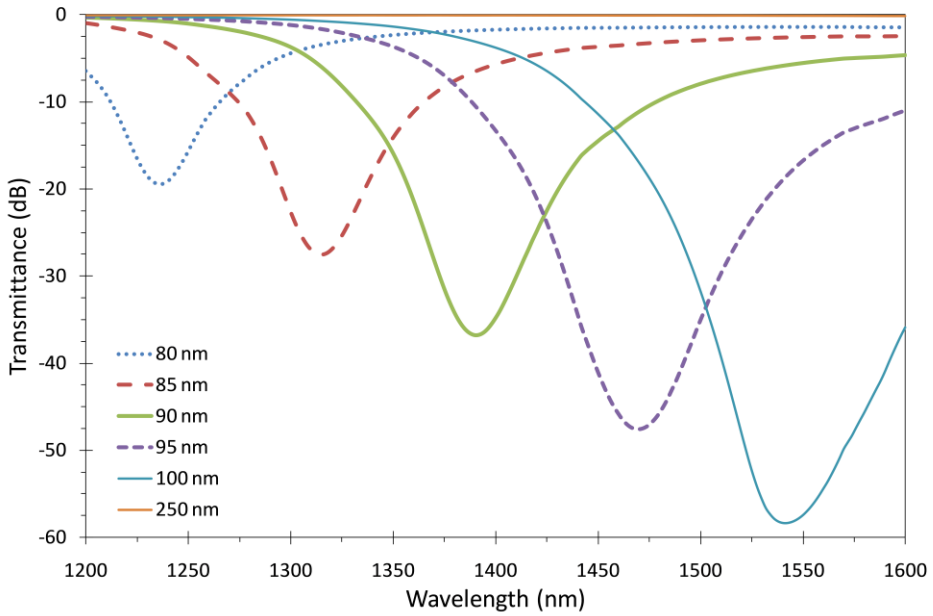

Fig. 6. Numerical spectra for different ITO thin-film thickness values. Thickness of the cladding region between the core and the ITO coating: 5.2 µm. ITO thin-film length 17 mm. SRI= 1.321.

In Fig. 7 the wavelength shift of the LMRs is presented both experimentally and theoretically for several refractive indices around a refractive index of 1.321, the typical value of aqueous solutions. The sensitivity obtained is 5,855 nm per refractive index unit (nm/RIU).

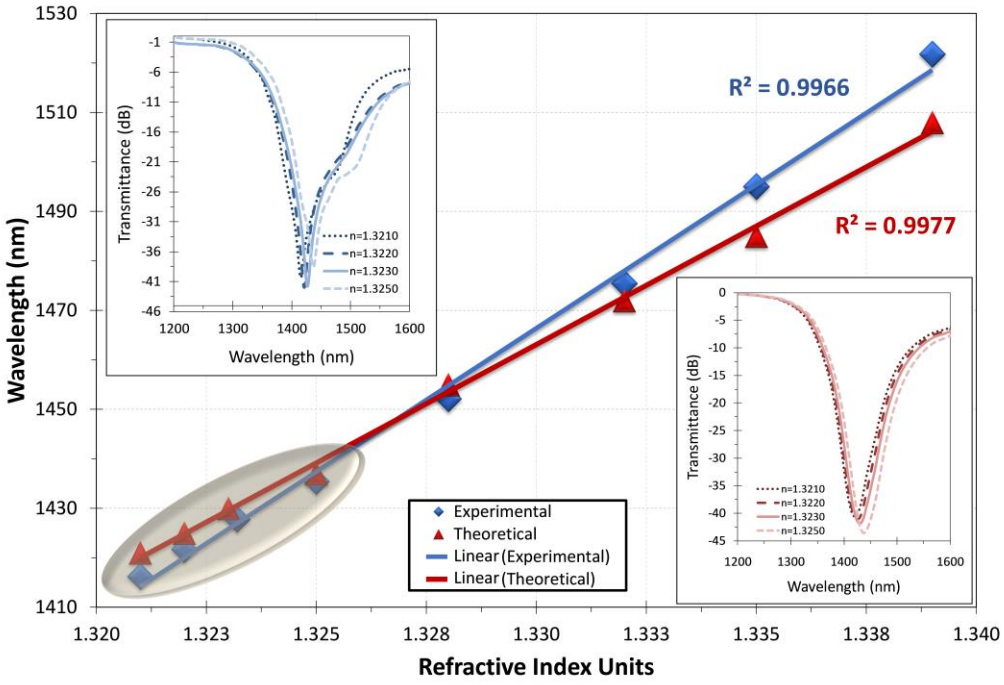

Fig. 7. Numerical and experimental wavelength shift of the LMR for different refractive indices around 1.321 (aqueous solutions). R-squared is a statistical measure that shows how close the data are to the fitted linear regression lines in the figure.

In Fig. 8, the electric field intensity in the transversal section of the D-shaped fiber is represented at different wavelengths for the fundamental mode ($HE_{1,1}$) and for one of the cladding modes that experience a transition to guidance in the ITO layer ($TE_{1,1}$). The mode $TE_{1,1}$ is initially confined in the cladding of the optical fiber at 1690 nm. However, it experiences a transformation into a TE mode in the ITO layer as the wavelength decreases. Regarding $HE_{1,1}$, it is confined in all cases in the fiber core. Nonetheless, it is remarkable to mention that at 1420 nm there is a region, in the proximity of the thin-film, with a subtle yellower color. This

indicates that part of the power transmitted by the core mode is coupled to the ITO thin-film, which corresponds to the LMR and corroborates the authors' claims.

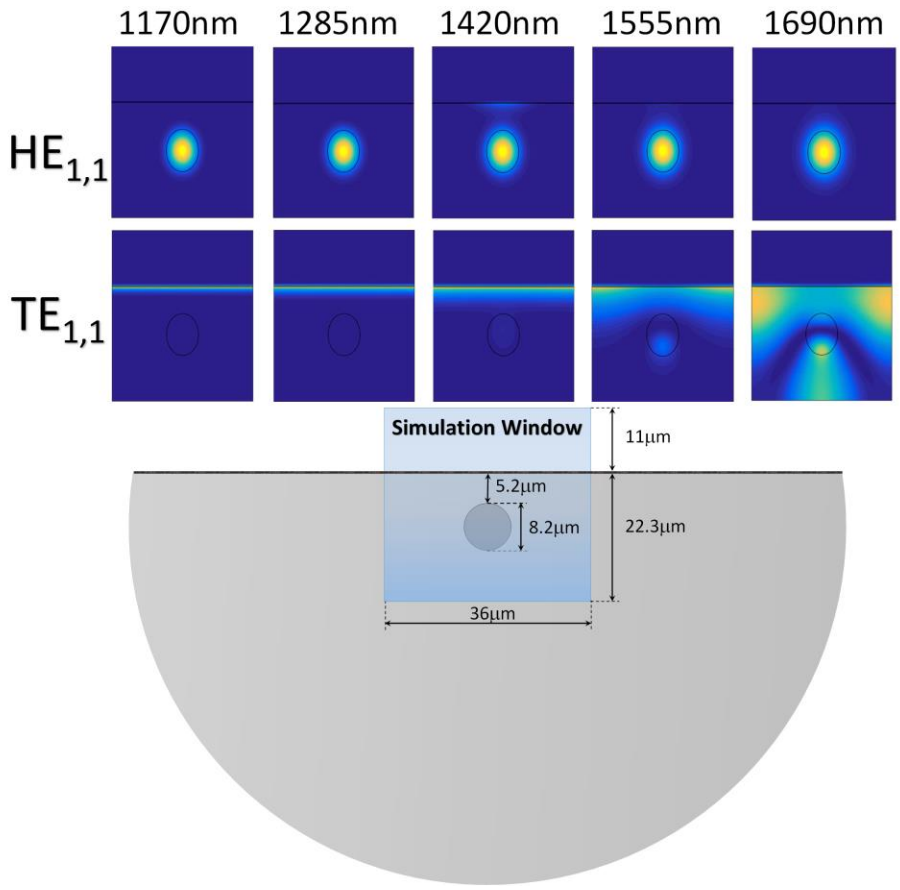

Fig. 8. Electric field intensity in the transversal section of the ITO coated D-shaped fiber. The simulation window is indicated on the schematic of the D-shaped fiber, in the center of the figure. The fundamental mode $HE_{1,1}$ and the first mode that experiences a transition to guidance in the overlay ($TE_{1,1}$), are analyzed for different wavelengths. As the wavelength decreases $TE_{1,1}$ is progressively confined in the ITO thin-film.

In addition, in the video included as supplementary material, S1, the progressive visualization of the electric field intensity as the wavelength decreases, permits to observe clearly that in the proximity 1420 nm there is a modification in $HE_{1,1}$ due to the $TE_{1,1}$ transition. This coincides again with the LMR wavelength region.

Some design rules can be used towards the optimization of the sensitivity of LMR based sensors [16]. The first one is to choose the first LMR (i.e. the LMR that is produced by the transition of

the first TE mode). This is the case in the results presented so far. However, there are two other important ways to increase the sensitivity.

The first one consists of increasing the SRI approaching the refractive index of the substrate, in this case the optical fiber. In Fig. 9, on the right, results are presented of another D-shaped fiber coated with an ITO layer but characterized for refractive indices in the range 1.4474-1.449.

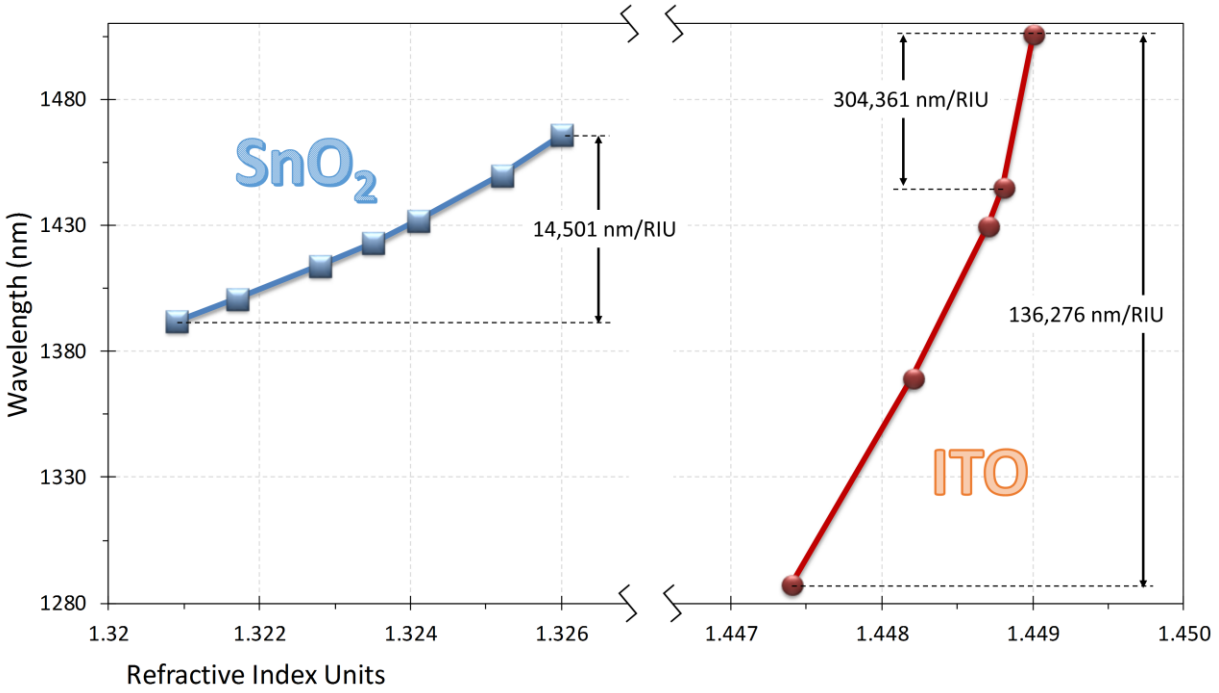

Fig. 9. Experimental central wavelength of the LMR for two different refractive index ranges (the water region and the 1.4474-1.449 region) and two different moderate absorbing thin-film materials: SnO_2 and ITO. Please note that the horizontal scale is not the same for both regions.

The sensitivity achieved is 136,276 nm/RIU. This overcomes, by factor of 23, the value obtained in the range of 1.321-1329. Moreover, in the narrower range 1.4487-1.449 a 304,361 nm/RIU, a 52-fold increase is attained.

However, in order to obtain chemical sensors or a biosensors, the region of interest is the water region, where the analysis of the sensitivity indicates the quality of the sensor developed further [24]. The sensitivity obtained with the ITO thin-film is 5,855 nm/RIU. In order to improve this, we apply extract the second rule indicated in [18]: to increase the refractive index of the thin-film. To this purpose, a different device is fabricated using a SnO_2 coating deposited on

another D-shaped fiber. The sensitivity in the water region (refractive index around 1.321) is 14,510 nm/RIU (see Figure 9). This is nearly 3 times more than the value obtained with the ITO layer.

This record sensitivity improves the highest sensitivity reported with long-period fiber gratings (LPFG), 9,100 nm/RIU [25], that attained with localized surface plasmon resonance by a factor of 70 [26], and our previous results with D-shaped fiber by a factor of 4 [19]. Moreover, even though the sensitivity is lower than photonic crystal fiber [27] and SPRs [28], the application of higher refractive index materials in future works should permit to compete with these last two technologies. Regarding commercial devices, biosensing label free technology has been used by several companies focused on biosensing: Biacore http://www.biacore.com, Bionavis http://www.bionavis.com, or PC Biosensors http://www.pcbiosensors.com. Actually, with the comparison table indicated in [29], Biacore T200 and EVA 2.0 from PCbiosensors are the two most sensitive devices with $3x10^{-8}$ is and $5x10^{-8}$ RIU resolution respectively. Our D-shaped fiber monitored with an Optical Spectrum Analyzer (OSA) with 1 pm resolution presents a resolution that improves these values: 3.28×10^{-9} RIU, and is better than the rest of devices analyzed: Biacore X100, OWLS 210 and Horiba OpenPlex.

A final way of improving the performance of D-shaped fiber devices could be to apply reversed symmetric waveguides [30]. By changing the substrate material we could obtain the same sensitivity obtain in the silica refractive index region for the water region.

4. CONCLUSIONS

It has been proved with an ITO nanocoated D-shaped fiber that a record sensitivity of 304,360 nm can be obtained by adequate selection of the surrounding medium refractive index. This value overcomes the detection limits of all other optical devices: surface plasmon resonance sensors, long period fibre gratings or photonic crystal fiber, and could become a reality for the water region if the substrate refractive index is reduced, like in reserved symmetric waveguides. Another option is to choose, instead of ITO, a higher refractive index material such as SnO2, which in this article permits to improve the sensitivity by a factor of 3.

In spite of being in the early stages of LMR devices, the first experimental demonstrations of LMR sensors have been already reported: refractometers [6,18], gas sensors [31], pH sensors [32], humidity sensors [33], or inmunosensors [34]. Moreover, the record sensitivity presented here indicates that the utilization of LMR can be a very competitive alternative for designing instrumentation devices that require an extremely high sensitivity. This can have a high impact in diverse disciplines such as those related to life sciences.

ACKNOWLEDGEMENTS:

This work was supported in part by the Spanish Ministry of Economy and Competitiveness (MINECO)-under contract FEDER TEC2013-43679-R. Special thanks to Horiba Scientific, Thin Film Division for the spectrometric ellipsometry characterization of the samples.

References:

1. T. E. Batchman, G. M. McWright, “Coupling Between Dielectric and Semiconductor Planar Waveguides,” IEEE J. Quant. Electron. QE-18 (1995), 782-788.
2. M. Marciniak, J. Grzegorzewski, M. Szustakowski, “Analysis of lossy mode cut-off conditions in planar waveguides with semiconductor guiding layer,” IEE Proceedings. Part J, Optoelectronics 140 (1993), 247-252.
3. N. Skivesen, R. Horvath, H.C. Pedersen Skivensen “Optimization of metal-clad waveguide sensor,” Sens. Actuators B, 106 (2005), 668-676.
4. F. Poletti, N. V. Wheeler, M. N. Petrovich, N. Baddela, J. Numkam Fokoua, R. Hayes, D. R. Gray, Z. Li, R. Slavík, D. J. Richardson, “Towards high-capacity fibre-optic communications at the speed of light in vacuum,” Nature Photon. 7 (2013), 279–284.
5. A. G. Brolo, “Plasmonics for future biosensors,” Nature Photon. 6 (2012), 709–713.
6. I. Del Villar, C. R. Zamarreño, M. Hernaez, F. J. Arregui, I. R. Matias, “Lossy Mode Resonance Generation with Indium-Tin-Oxide-Coated Optical Fibers for Sensing Applications,” J. Lightwave Technol. 28 (2010), 111-117.
7. F. Yang, J. R. Sambles, “Determination of the optical permittivity and thickness of absorbing films using long range modes,” J. Mod. Opt. 44 (1997), 1155-1563.
8. D. Razansky, P. D. Einziger, D. R. Adam, “Broadband Absorption Spectroscopy via Excitation of Lossy Resonance Modes in Thin Films,” Phys. Rev. Lett. 95 (2005), 018101.

9. N. Paliwal, J. John, “Theoretical modeling of lossy mode resonance based refractive index sensors with ITO/TiO2 bilayers,” Appl. Opt. 53 (2014), 3241-3246.
10. D. Kaur, V. K. Sharma, A. Kapoor, Sens. Actuators, “High sensitivity lossy mode resonance sensors,” Sens. Actuators, B 198 (2014), 366-376.
11. M. Hernaez, C. R. Zamarreño, I. R. Matias, F. J. Arregui, “Optical fiber humidity sensor based on surface plasmon resonance in the infra-red region,” SPIE Proceedings 7503 (2009), 75030L.
12. S. K. Mishra, S. Rani, B. D.Gupta, “Surface plasmon resonance based fiber optic hydrogen sulphide gas sensor utilizing nickel oxide doped ITO thin film,” Sens. Actuators, B 195 (2014), 215-222.
13. M. Rani, N. K. Sharma. V. Sajal, “Surface plasmon resonance based fiber optic sensor utilizing indium oxide,” Optik 124 (2013), 5034-5038.
14. I. Del Villar, V. Torres, and M. Beruete, “Experimental demonstration of lossy mode and surface plasmon resonance generation with Kretschmann configuration,” Opt. Lett. 40 (2015), 4739–4382.
15. V. Torres, and M. Beruete, P. Sanchez and I. Del Villar, “Indium tin oxide refractometer in the visible and near infrared via lossy mode and surface plasmon resonances with Kretschmann configuration,” Appl. Phys. Lett. 108 (2016), 043507.
16. C. Rhodes, S. Franzen, J. P. Maria, M. Losego, D. N. Leonard, B. Laughlin, G. Duscher and S. Weibel, “Surface plasmon resonance in conducting metal oxides,” Appl. Phys. Lett. 100 (2006), 054905.
17. S. Franzen, C. Rhodes, M. Cerruti, R.W. Gerber, M. Losego, J.P. Maria, D. E. Aspnes, “Plasmonic phenomena in indium tin oxide and ITO–Au hybrid films,” Opt. Lett. 34 (2009), 2867-2869.
18. I. Del Villar, M. Hernaez, C. R. Zamarreño, P. Sanchez, C. Fernandez-Valdivielso, F. J. Arregui, I. R. Matias, “Design rules for lossy mode resonance based sensors,” Appl. Opt. 51 (2012), 4298-4307.
19. P. Zubiate, C. R. Zamarreño, I. Del Villar, I. R. Matias, F.J.Arregui, “High sensitive refractometers based on lossy mode resonances (LMRs) supported by ITO coated D-shaped optical fibers,” Opt. Express, 23 (2015), 8045-8050.
20. I. H. Malitson, “Comparison of the Refractive Index of Fused Silica,” J. Opt. Soc. Am. 55 (1965), 1205-1209.
21. G. M. Hale and M. R. Querry. Optical Constants of Water in the 200-nm to 200-µm Wavelength Region, Appl. Opt. 12, 555-563 (1973)
22. P. R. Cooper, “Refractive-index measurements of liquids used in conjunction with optical fibers,” Appl. Opt. 22, 3070–3072 (1983).

23. I. Del Villar, I. R. Matias, F. J. Arregui, M. Achaerandio, “Nanodeposition of Materials With Complex Refractive Index in Long-Period Fiber Gratings,” IEEE J. Lightwave Technol. 23, 4192-4199 (2005).

24. F. Chiavaioli, P. Biswas, C. Trono, S. Bandyopadhyay, A- Giannetti, S. Tombelli, N. Basumallick, K. Dasgupta, and F. Baldini, “Towards sensitive label-free immunosensing by means of turn-around point long period fiber gratings,” Biosens. Bioelectron. 60, (2014), 305–310.

25. P. Pilla, C. Trono, F. Baldini, F. Chiavaioli, M. Giordano, and A. Cusano, “Giant sensitivity of long period gratings in transition mode near the dispersion turning point: an integrated design approach,” Opt. Lett. 37 (2012), 4152-4154.

26. J. N. Anker, W. P. Hall, O. Lyandres, N. C. Shah, J. Zhao, R. P. Van Duyne, “Biosensing with plasmonic nanosensors,” Nature Materials 7 (2008), 442-453.

27. D. K. C. Wu, B. T. Kuhlmey, B. J. Eggleton, “Ultrasensitive photonic crystal fiber refractive index sensor,” Opt. Lett. 4 (2009), 322-324.

28. R. Slavík, J. Homola, “Ultrahigh resolution long range surface plasmon-based sensor,” Sens. Actuators, B 123 (2007), 10-12.

29. Comparsion table of biosensors by PCbiosensors: http://www.pcbiosensors.com/biosensors_comparison_table/table_OWLS_SPR_PCSW.pdf

30. R. Horváth, L. R. Lindvold, N. B. Larsen, “Reverse-symmetry waveguides: theory and fabrication,” Appl. Phys. B 74 (2002), 383–393.

31. S. P. Usha, S. K. Mishra, B. D. Gupta, “Fiber optic hydrogen sulfide gas sensors utilizing ZnO thin film/ZnO nanoparticles: A comparison of surface plasmon resonance and lossy mode resonance,” Sens. Actuators, B 218 (2015), 196-204.

32. C. R. Zamarreño, M. Hernaez, I. Del Villar, I. R. Matias, F. J. Arregui, “Optical fiber pH sensor based on lossy-mode resonances by means of thin polymeric coatings,” Sens. Act. B. 155 (2011), 290-297.

33. P. J. Rivero, A. Urrutia, J. Goicoechea, F. J. Arregui, “Optical fibre humidity sensors based on localized surface plasmon resonance (LSPR) and lossy-mode resonance (LMR) in overlays loaded with silver nanoparticles,” Sens. Act. B, 173 (2012), 244-249.

34. A. B. Socorro, J. M. Corres, I. Del Villar, F. J. Arregui, I. R. Matias, “Fiber-optic biosensor based on lossy mode resonances,” Sens. Act. B, 174 (2012), 263-269.